

We are IntechOpen, the world's leading publisher of Open Access books Built by scientists, for scientists

6,900

Open access books available

186,000

International authors and editors

200M

Downloads

Our authors are among the

154

Countries delivered to

TOP 1%

most cited scientists

12.2%

Contributors from top 500 universities



WEB OF SCIENCE™

Selection of our books indexed in the Book Citation Index
in Web of Science™ Core Collection (BKCI)

Interested in publishing with us?
Contact book.department@intechopen.com

Numbers displayed above are based on latest data collected.
For more information visit www.intechopen.com



Remote Sensing of Atmospheric Trace Gases by Ground-Based Solar Fourier Transform Infrared Spectroscopy

Clare Paton-Walsh
University of Wollongong
Australia

1. Introduction

The changing composition of the earth's atmosphere is a matter of intense scientific research as we strive to understand details of the physical and chemical mechanisms that control our climate. Fourier transform spectroscopy has been applied very successfully to the study of trace gases in the atmosphere by examining terrestrial atmospheric absorption lines in the infrared spectrum from the Sun. In fact many gases were first discovered in the atmosphere during the 1940's from their absorption features in the infrared solar spectrum. These early optical absorption measurements of the atmosphere using the Sun as a source were made with grating spectrometers and examples of atmospheric gases first detected this way include methane and carbon monoxide (*Migeotte, 1948; 1949*).

Continuous or semi-continuous records of infrared solar atmospheric absorption spectra have been made from ground-based Fourier transform spectrometers (FTS) since the late 1970s and early 1980s, when the first ground-based solar-tracking FTS systems were installed at Kitt Peak National observatory in the USA and at the Jungfraujoch Observatory in Switzerland (*Goldman et al., 1979; Murcray et al., 1978; Zander et al., 1977*). Initially interest was focused on the detection and quantification of stratospheric trace gases (*Rinsland et al., 1986; Zander et al., 1986*). The discovery of the Antarctic ozone hole (*Farman et al., 1985*) intensified interest in stratospheric chemistry and helped support the establishment of the Network for Detection of Stratospheric Change (NDSC). This global network of instrument sites became operational in 1991 with ground-based FTS amongst the suite of primary techniques being used. Photographs of the instrument at the NDSC site at Wollongong, Australia are shown for illustrative purposes in figure 1 below. Other NDSC instruments are lidars for ozone, temperature, water and aerosols; microwave instruments for ozone, water and chlorine monoxide; UV/Visible spectrographs for ozone and nitrogen dioxide; Dobson/Brewer spectrophotometers for total column ozone and regular ozone sondes. The establishment of the NDSC resulted in a huge increase in the number of infrared solar absorption measurements being made around the globe during the next few years.

More recently interest in atmospheric chemistry has been focused on tropospheric pollution and anthropogenic emissions of greenhouse gases (*Barret et al., 2003; Jones et al., 2009; Mahieu et al., 1995; Nagahama and Suzuki, 2007; Paton-Walsh et al., 2008; Rinsland et al., 2000; Rinsland et al., 2001; Rinsland et al., 2002; Rinsland et al., 2008; Warneke et al., 2006; Zhao et al., 2000; Zhao*



Fig. 1. The ground-based solar Fourier Transform infrared spectrometer at Wollongong, Australia. The sun's radiation is captured by the solar tracker (shown above) and sent to the entrance optics of the high resolution Fourier transform spectrometer in the laboratory below (shown right). (Photography by R Macatangay)

et al., 2002). As a result, the NDSC has changed its emphasis and name to the Network for Detection of Atmospheric Composition and Change (NDACC) - see <http://www.ndacc.org/>. As well as an ever increasing number of sites in the global network the new millennium has seen an expansion into the near infrared spectra region in

an effort to provide extremely accurate and precise measurements of carbon dioxide and other greenhouse gases. The Total Column Carbon Observing Network (TCCON) was established to help characterise biogenic and oceanic sources and sinks of greenhouse gases to and from the atmosphere and to validate current and future satellite based measurements (<http://www.tcon.caltech.edu/>).

2. Atmospheric solar infrared Fourier transform transmission spectra

Fourier transform infrared spectroscopy is a powerful tool for monitoring the changing composition of the atmosphere because it can measure so many different gases simultaneously. The ability to measure atmospheric trace gases in the infrared is enhanced by the fact that the major components of the atmosphere (nitrogen, oxygen and argon) have no dipole moment and thus are infrared inactive.

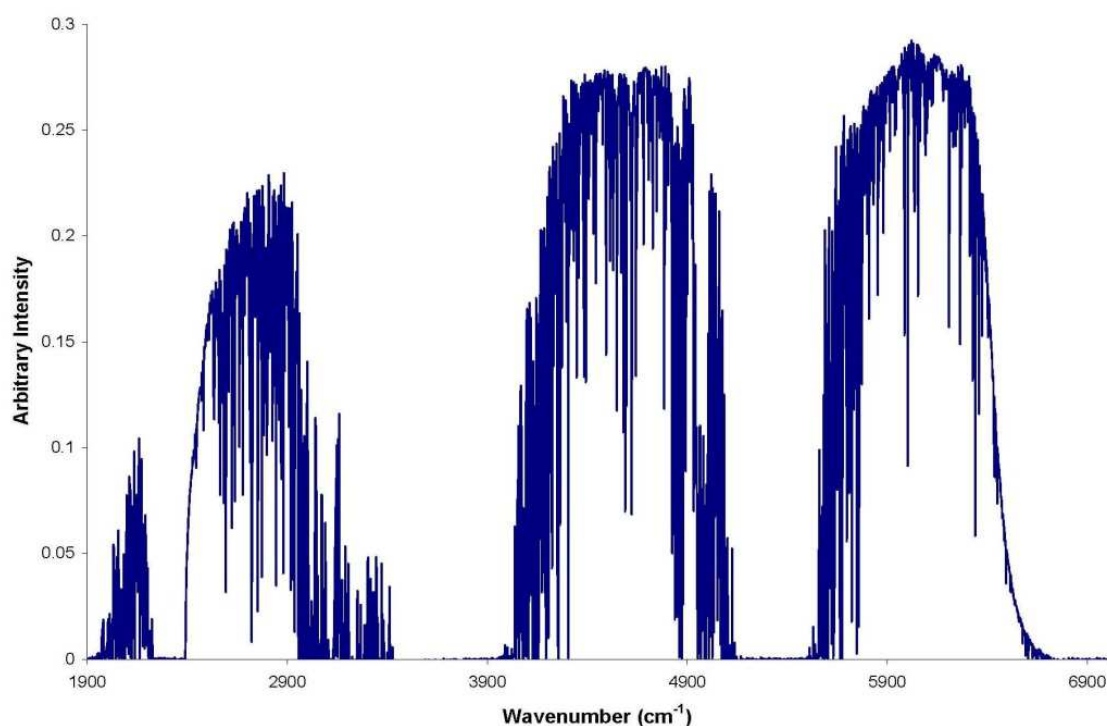


Fig. 2. An example spectrum recorded by a ground-based solar Fourier transform spectrometer

In ground-based solar Fourier transform spectroscopy, the Sun acts as the radiation source and the sample is the atmosphere. The shape of the resulting spectrum depends upon the solar radiation reaching the top of the Earth's atmosphere, absorption by the atmosphere and the optical properties of instrument recording the radiation. The solar radiation reaching the top of the Earth's atmosphere is in essence a blackbody curve at 5800K with emission and absorption lines of gases in the solar atmosphere imposed. Terrestrial atmospheric absorption lines contain information about the species of trace gases present in the atmosphere (line positions), the amounts of each gas present (line depths/areas) and some information about the altitude distribution of each gas (line shapes). In reality there is also a component of radiation as a result of atmospheric emission, but this is so small in comparison to the radiation from the sun that its effects are negligible.

3. Calculating synthetic solar atmospheric transmission spectra

Clearly it is not possible to measure a background spectrum or a set of calibration spectra when the atmosphere is the sample. For this reason the analysis of these spectra requires the calculation of a synthetic spectrum using a database of absorption line parameters such as the HITRAN database (Rothman *et al.*, 1998; Rothman *et al.*, 2003; Rothman *et al.*, 2005) and a model of the atmospheric conditions such as pressure, temperature and gas concentrations that all vary with altitude. The calculation must also take into account instrumental effects such as line shape and resolution.

The HITRAN (HIGH resolution TRANsmission) database contains calculated quantum mechanical parameters that describe the vibrational-rotational transitions of the most common atmospheric molecules. Parameters include the line positions (frequencies of absorption lines), line strengths at a reference temperature and pressure, lower state energy and pressure broadening and shift parameters.

3.1 Atmospheric absorption line positions

The characteristic absorption features seen in Figure 2 are caused by molecules absorbing radiation at frequencies that correspond to the allowed transitions between different vibrational and rotational states. The frequencies at which molecules absorb are determined by the allowed transitions between energy levels of the molecule and provide a unique identifier of trace gases in the atmosphere. Vibrational energy states are much more widely spaced than rotational energy states and so the line position is determined mainly by the change in vibrational state with small frequency differences depending on the accompanying change in rotational energy.

The energy of allowed states of a simple diatomic molecule can be approximated by Equation 1:

$$E = \hbar \sqrt{\frac{k}{\mu}} \left(v + \frac{1}{2} \right) + BJ(J+1) \quad (1)$$

(if it is assumed that molecule behaves like a simple harmonic oscillator and a rigid rotor) and where:

- \hbar is Planck's constant divided by 2π ,
- k and μ are the force constant and the reduced mass of the molecule respectively,
- B is the rotational constant ($B = \hbar^2 / 2I$, where I is the moment of inertia, the product of the reduced mass and the square of the radius of rotation)
- and v and J are the vibrational quantum number and rotational quantum number of the state respectively.

For diatomics the allowed transitions between states are $\Delta v = \pm 1, \pm 2, \pm 3, \dots$ and $\Delta J = \pm 1$.

A vibration-rotation transition with $\Delta v = -1$ results in an *emission* spectrum and a transition with $\Delta v = +1$ an *absorption* spectrum, and both types of spectra may be accompanied by either a gain in rotational energy $\Delta J = +1$ or a loss in rotational energy $\Delta J = -1$. This produces a spectrum with two branches, one either side of the pure vibrational frequency, ν_0 . The R branch corresponds to a vibrational transition accompanied by a gain in rotational energy $\Delta J = +1$ and consists of a set of lines spaced approximately $2B$ apart to the high frequency side of the pure vibrational frequency, ν_0 , becoming more closely packed as the rotational energy increases further from the band centre, (assuming $B_1 < B_0$). The P branch corresponds

to a vibrational transition accompanied by a loss in rotational energy $\Delta J = -1$ and consists of a set of lines spaced approximately $2B$ apart to the low frequency side of the pure vibrational frequency, ν_0 , becoming more widely spaced as the rotational energy increases away from the band centre. Linear polyatomic molecules can also vibrate in a manner such that the dipole moment is changed perpendicular to the principal axis of rotational symmetry and in this case the selection rules also allow $\Delta J = 0$, i.e. the vibrational energy change can occur without an accompanying change in rotational energy. In such spectra the Q-branch appears at the band centre between the P and R branches (at the pure vibrational frequency, ν_0). The Q-branch is a relatively intense feature because the vibrational transitions occur from all existing rotational states with approximately the same energy change and hence the same frequency.

3.2 Line broadening and line shapes

As a consequence of Heisenberg's uncertainty principle, absorption lines are never infinitely narrow. The uncertainty in the energy of a state multiplied by the uncertainty in time (the lifetime of a state) must be greater or equal to \hbar , ($\Delta E \Delta t > \hbar$). So the shorter the lifetime, the larger the uncertainty in a state's energy and the broader the absorption or emission line (as the energy uncertainty manifests itself as an uncertainty in the frequency of the line). Uncertainty broadening due to the radiative or intra-molecular lifetime of the state in isolation is always present but for vibrational-rotational states is usually very small ($< 10^{-6} \text{ cm}^{-1}$). Another form of uncertainty broadening, which dominates at atmospheric pressures, is collisional broadening (also called pressure broadening) and occurs when the collisions of atoms, ions or gas molecules shorten the lifetime of states. In gases it is proportional to pressure and this means that absorption lines from spectra taken through the whole atmosphere will have different shapes depending upon the distribution of the absorbing gas in the atmosphere. A gas that is mainly located in the troposphere (such as methanol) will display broad absorption lines because of the high pressure whilst predominantly stratospheric gases (like ozone) will produce much narrower lines since the pressure is low. Uncertainty broadening leads to a Lorentzian line shape contribution at a given wavenumber ν :

$$f_L(\nu) = \frac{\alpha_L / \pi}{(\nu - \nu_0)^2 + \alpha_L^2} \quad (2)$$

where:

- ν_0 is the absorption line frequency in wavenumbers, and
- α_L is the Lorentzian half-width at half height, which is proportional to the total pressure.

Absorption lines due to atmospheric gases are also subject to Doppler broadening. Doppler broadening occurs because molecules that travel with different velocities with respect to the light source, absorb at different wavelengths, just as light from stars accelerating away from the Earth is red-shifted. Doppler broadening produces a Gaussian line shape due to the Gaussian distribution of molecular velocities:

$$f_G(\nu) = \frac{1}{\alpha_G \sqrt{\pi}} \exp\left(-\frac{(\nu - \nu_0)^2}{\alpha_G^2}\right) \quad (3)$$

where

- α_G is the Gaussian half-width at half height and is given by:

$$\alpha_G = \frac{v_l}{c} \sqrt{\frac{2kT}{m}} \quad (4)$$

where

- k is the Boltzmann constant,
- T is the Kelvin temperature and
- m is the molecular mass.

Pressure broadening (with Lorentzian lineshape) dominates in the troposphere¹, but its effects drop off rapidly with altitude as the pressure drops. Doppler broadening (with Gaussian line shape) is temperature dependent but its variation through the atmosphere is much smaller than pressure broadening. Stratospheric gas lines are primarily Doppler broadened and the two types of broadening become equally significant at around 25 km. The convolution of Lorentzian and Gaussian line shapes produces a Voigt line shape. This variation of the shape and width of absorption lines with the pressure of the absorbing gas means that spectra of atmospheric gases contain information about the altitude of the absorbing gas as well as the total number of absorbing molecules in the path.

3.3 Atmospheric absorption line intensities

The integrated line strength of each absorption line of each molecule is determined by the transition probability, the population and degeneracy of the initial state and the number of absorbing molecules in the path. In local thermodynamic equilibrium the population of states is determined by the Boltzmann distribution, which is dependent upon the temperature of the absorbing molecules and for this reason line strengths are temperature dependent.

At a given wavenumber (ν), the intensity of radiation (the radiative power) that reaches the ground $I(\nu)$, is related to the radiative power at the top of the atmosphere $I_0(\nu)$ by Equation 5:

$$I(\nu) = I_0(\nu)e^{-m\tau(\nu)} \quad (5)$$

where

- $\tau(\nu)$ is the *optical depth* of the atmosphere and
- m is the *airmass factor* - a geometrical factor accounting for the slant path through the atmosphere.

In order to calculate a synthetic spectrum all molecules that absorb in the spectral region being simulated must be considered together. At any given wavenumber (ν), the contribution to the optical depth (τ) for every absorption line k of each molecule i , is given by

$$\tau_i^k(\nu) = \sigma_i^k(\nu) \cdot a_i \quad (6)$$

where

- $\sigma_i^k(\nu)$ is the absorption coefficient or cross section at

¹ Typical values for a mid-size molecule are $\alpha_L \sim 0.15 \text{ cm}^{-1} \text{ atm}^{-1}$ and $\alpha_G \sim 0.004 \text{ cm}^{-1}$.

- ν , for each absorption line k of each molecule i , (typically in units $\text{cm}^2 \text{molec}^{-1}$)
- a_i is the amount of molecule i , in units of molec cm^{-2} .

The absorption coefficient $\sigma_i^k(\nu)$ is the convolution (\otimes) of the integrated line strength, S_i^k and the pressure broadening and Doppler broadening line-shapes:

$$\sigma_i^k(\nu) = S_i^k \otimes [f_L(\nu)]_i^k \otimes [f_G(\nu)]_i^k \quad (7)$$

The HITRAN 2004 database contains line parameters for 39 atmospheric gases including the wavenumber of each absorption line, the integrated line strengths at 296K, the lower state energy E_0 , the air-broadened Lorentzian half-width at atmospheric pressure and its temperature dependence.

The integrated line strength is temperature dependent because of the temperature dependence of the population of the lower-state energy and a small contribution from the spontaneous emission. The integrated line strength at any given temperature (S_T) may be calculated using the integrated line strengths at 296K and other parameters given in HITRAN with Equation 8:

$$S(T) = S(296) \frac{Q(296)}{Q(T)} \cdot \frac{\exp(-\frac{c_2 E_0}{T})}{\exp(-\frac{c_2 E_0}{296})} \cdot \frac{(1 - \exp(-\frac{c_2 \nu_0}{T}))}{(1 - \exp(-\frac{c_2 \nu_0}{296}))} \quad (8)$$

where

- $Q(296)$ and $Q(T)$ are the partition functions at these temperatures and
- c_2 is the second radiation constant, ($c_2 = hc/k = 1.439 \text{ cm K}$) (Griffith, 1996).

3.4 Calculating synthetic solar atmospheric transmission spectra

The dry atmosphere is composed of mainly nitrogen (78%) and oxygen (21%) with minor and trace gases making up the other 1%. The normal modes of vibration of nitrogen and oxygen are infrared inactive because the symmetry of the molecules is such that vibrations do not cause a change in the dipole moment, so there is nothing for incoming infra-red radiation to interact with. Thus the main constituents of the atmosphere transmit infra-red radiation and the infrared spectrum of the atmosphere as shown in Figure 2 is dominated by minor constituents and trace gases such as water, carbon dioxide and methane. This is the reason that these species are important greenhouse gases.

The temperature, pressure and concentrations of trace gases in the atmosphere change continuously with altitude. In order to calculate a synthetic spectrum the atmosphere is modelled as a series of homogeneous layers each with a defined temperature, pressure and gas composition². To model the radiative transfer through the atmosphere the path length of radiation from the sun through each layer of the modelled atmosphere must be calculated using a ray-tracing algorithm that takes into account the solar zenith angle at the time of the

² The amounts of atmospheric trace gases are often measured in mole ratios, defined as the number of moles of the substance of interest per mole of air. For trace gases the usual units are micro moles per mole ($\mu\text{mol.mol}^{-1}$) – sometimes expressed as parts per million (ppm), e.g. 5 ppm CO means 5 molecules of carbon monoxide per million molecules of air). For ultra-trace gases the units often used are nano moles per mole (nmol.mol^{-1}) or picomoles per mole (pmol.mol^{-1}).

measurement and the effects of atmospheric curvature and refraction. At least thirty different atmospheric layers are required in order to do the radiative transfer calculation without errors in this calculation becoming a dominant uncertainty (Meier *et al.*, 2003).

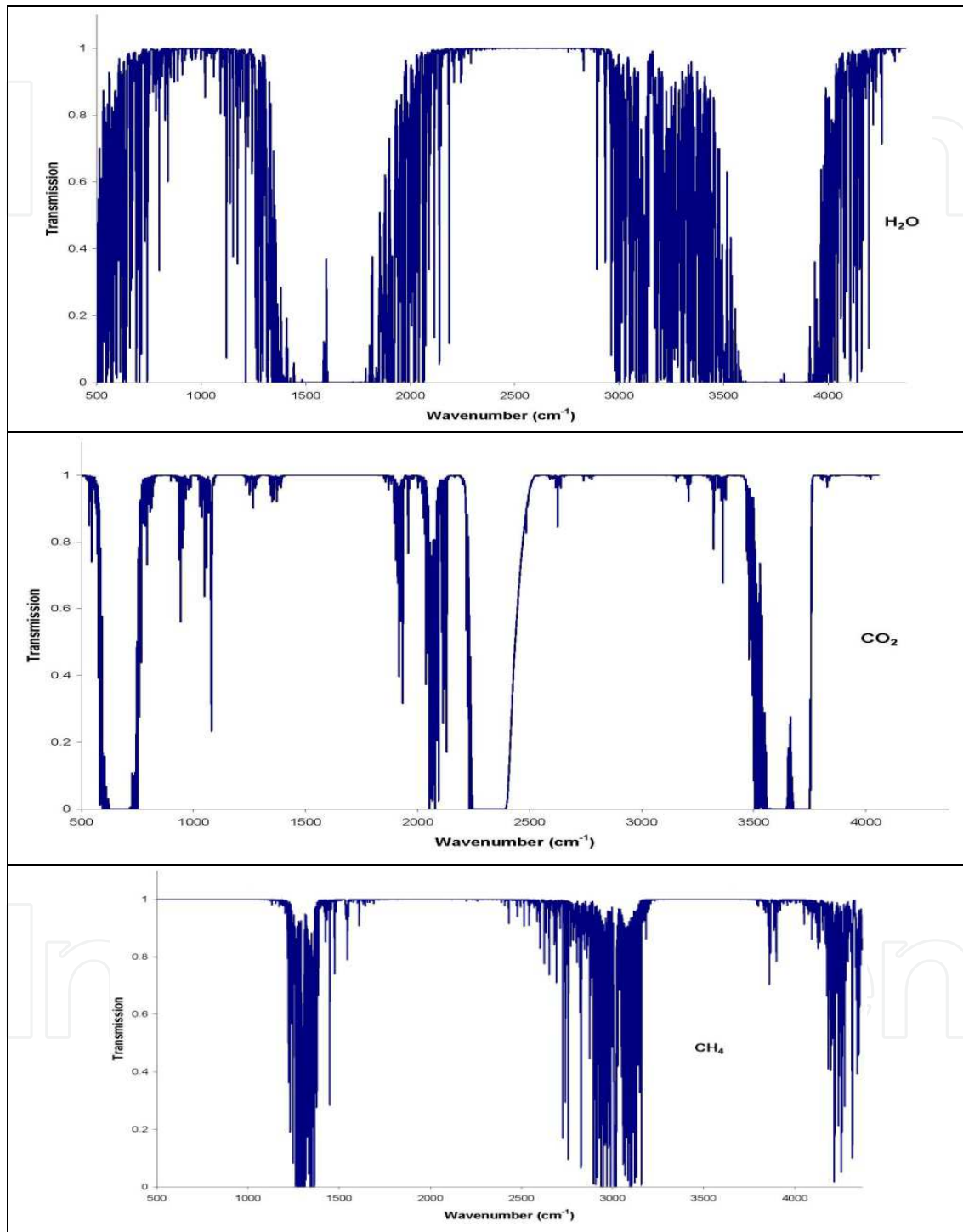


Fig. 3. The infrared transmission spectrum of water (top panel), carbon dioxide (middle panel) and methane (bottom panel) in the atmosphere from 500 cm⁻¹ to 4400 cm⁻¹ as simulated using the HITRAN 2000 database for a solar zenith angle of 70° and concentration profiles taken from US standard atmosphere (Meier *et al.*, 2004)

Following on from Equation 6, when all the absorption lines of all molecules are considered, the total optical depth at any given frequency, $\tau(\nu)$, is the sum of the contribution of all the absorption lines of all molecules, for all homogeneous layers:

$$\tau(\nu) = \sum_{\text{layers}} \sum_i \sum_k \tau_i^k(\nu) \quad (9)$$

The true atmospheric transmittance spectrum, $T(\nu)$ is the ratio of the intensity at the ground, $I(\nu)$, and the intensity at the top of the atmosphere, $I_0(\nu)$:

$$T(\nu) = \frac{I(\nu)}{I_0(\nu)} = \exp(-\tau(\nu)) \quad (10)$$

The calculation of the synthetic spectrum must also include the effects of instrumental parameters such as the resolution and instrumental line-shape including phase error and wavelength shift. The spectrum that will actually be measured is a convolution of the intensity at the ground, $I(\nu)$ and the instrumental line-shape. The instrumental line-shape (ILS) may be derived using measurements of low-pressure gas cells (Hase *et al.*, 1999), or a theoretical ideal ILS can be calculated from the instrument's field of view, resolution and the apodisation function³.

Example simulations calculated in this manner are shown in Figure 3 (Meier *et al.*, 2004). In these cases the infrared transmission spectra that result from just one component atmospheric gas at a time are given, namely water, carbon dioxide and methane. The spectra are simulated from 500 cm^{-1} to 4400 cm^{-1} using the HITRAN 2000 database for a solar zenith angle of 70° and concentration profiles taken from US standard atmosphere.

4. Theoretical basis for the retrieval of trace gas amounts from atmospheric solar infrared Fourier transform transmission spectra

4.1 Development of analysis algorithms

Over the years several different analysis algorithms have been developed to perform the retrieval of trace gas amounts from solar FTIR spectra. All the techniques calculate a synthetic spectrum using a "forward model" as described above, that includes a model of the instrumental effects and a layered model of the atmosphere with assumptions about environmental parameters such as the pressure, temperature and composition of each layer. The synthetic spectrum is compared to the measured spectrum and adjustments made to the forward model until a best fit with the measured spectrum is obtained.

Different analysis algorithms allow different adjustments to the forward model in order to achieve the best fit to the measurement.

- "SFIT1" (Rinsland *et al.*, 1982; Rinsland *et al.*, 1984) and "GFIT" (Washenfelder *et al.*, 2006) allow only a scaling of the *a priori* concentration profile of the absorbing gases to achieve best fit. This means that the distribution of the absorbing gas is defined entirely

³ An apodisation function is a mathematical function that is applied to the interferogram that may give greater weight to the information around zero path difference compared to information at greater optical path differences. In the analyses presented in this thesis a boxcar apodisation function was used that gives equal weight to the information throughout the interferogram.

by the *a priori* assumptions – the fitting process for example cannot put more gas in the troposphere and less in the stratosphere but must multiply the concentration in each of the modelled layers by the same multiplicative factor.

- Later development “SFIT2” (Pougatchev *et al.*, 1995) using optimal estimation techniques (Rodgers, 1990) aimed to extract the limited spectral information on the vertical distribution of the target gas, which is contained in the shape of the absorption features as a result of pressure broadening by the surrounding atmospheric gases (Hase *et al.*, 2004; Rinsland *et al.*, 1998).
- More recently another analysis code (“PROFITT”) has been developed using optimal estimation techniques that allows the temperature profile and concentration profiles to be adjusted (Hase *et al.*, 2004).

4.2 Inverse modelling and optimal estimation

In contrast to GFIT, SFIT2 allows the volume mixing ratio profile of the absorbing gas in the simulated spectrum to be adjusted so that the shape of the absorption line can best fit the measured spectrum. The principle difficulty in this technique is that the radiative transfer model requires at least thirty atmospheric layers to achieve a reasonable model of the transmission of solar radiation through the atmosphere, but the shape of an absorption feature typically contains between one and five independent pieces of information. Thus the problem is mathematically underdetermined and much of the information must still be provided by the *a priori* concentration profile in the forward model.

SFIT2 uses an inverse modeling technique (Rodgers, 1990; Rodgers, 2000) to extract the volume mixing ratio profile of the gases of interest from the measured spectrum. The volume mixing ratios of the gas of interest at each of the modeled layers are the variables of interest (called state variables or together the state vector \mathbf{x} , with n elements). The measured spectrum (a series of observed radiances at different frequencies) is represented by the observation vector \mathbf{y} (with m elements), and the forward model, F , describes the relationship between the observation vector \mathbf{y} (the spectrum) and the state vector \mathbf{x} , (the volume mixing ratios of the gases of interest).

$$y = F(x, b) + \varepsilon \quad (11)$$

where \mathbf{b} is a *parameter vector* including all model variables that are not to be optimized (also called the *model parameters*), and ε is the error vector including errors in the observations, in the forward model, and in the model parameters.

Inverting Equation 11, \mathbf{x} may be obtained given \mathbf{y} , but due to the error term ε the best that can be achieved is a statistical estimate. As stated before the problem is mathematically underdetermined and in optimal estimation \mathbf{x} is weighted by our prior (*a priori*) knowledge of the state vector \mathbf{x}_a (the *a priori* volume mixing ratio profile). The optimal solution of \mathbf{x} including this *a priori* knowledge is called the “*optimal estimate*” or the ‘*retrieval*’ (also sometimes called the “*a posteriori* solution”).

The *a priori* estimate has its own error: $\mathbf{x}_a = \mathbf{x} + \varepsilon_a$ and the key to solving the optimal estimation problem is weighting the error statistics of ε and ε_a (Rodgers, 2000).

The inverse problem lends itself to the use of matrix algebra, and the *Jacobian matrix*, \mathbf{K} , is a linearization of the forward model that represents the sensitivity of the observation variables \mathbf{y} to the state variables \mathbf{x} , assembled in matrix form (Jacob, 2007):

$$K = \nabla_x F = \frac{\partial y}{\partial x} \quad (12)$$

\mathbf{K} changes with \mathbf{x} and so it is calculated initially for the *a priori* value \mathbf{x}_a and then recalculated iteratively until the solution converges. The algorithm iterates until the cost function $J(\mathbf{x})$ is minimised by solving for $\nabla_x J(\mathbf{x}) = 0$ as shown in Equation 13:

$$\nabla_x J(\mathbf{x}) = 2S_a^{-1}(\mathbf{x} - \mathbf{x}_a) + 2K^T S_\epsilon^{-1}(K\mathbf{x} - \mathbf{y}) = 0 \quad (13)$$

where S_a and S_ϵ are the *a priori* error and observational error covariance matrices respectively (the matrix equivalents of ϵ_a and ϵ). Note that observational error includes errors in the forward model as well as spectral noise and that in many instances it is the forward model error that dominates the S_ϵ matrix.

The solution to Equation 13 yields the *optimal estimate* or *retrieval* $\hat{\mathbf{x}}$ and is given by Equation 14:

$$\hat{\mathbf{x}} = \mathbf{x}_a + G(\mathbf{y} - K\mathbf{x}_a) \quad (14)$$

where G is known as the *gain matrix* and describes the sensitivity of the retrieval to the observations, i.e. $G = \frac{\partial \hat{\mathbf{x}}}{\partial \mathbf{y}}$, and is given by Equation 15:

$$G = (K^T S_\epsilon^{-1} K + S_a^{-1})^{-1} K^T S_\epsilon^{-1} \quad (15)$$

4.3 Uncertainties in retrieved trace gas amounts and the “averaging kernel”

The ability of the measured spectrum to constrain the volume mixing ratio profile of the gas of interest, (the state vector, \mathbf{x}) is given by the *averaging kernel matrix* $A = \frac{\partial \hat{\mathbf{x}}}{\partial \mathbf{x}}$, which represents the sensitivity of the retrieval $\hat{\mathbf{x}}$ to the true state vector \mathbf{x} .

The *averaging kernel matrix*, $\mathbf{A} = \mathbf{GK}$, i.e. it is the product of the gain matrix $G = \frac{\partial \hat{\mathbf{x}}}{\partial \mathbf{y}}$ and the

Jacobian matrix $K = \frac{\partial \mathbf{y}}{\partial \mathbf{x}}$.

The information content may be defined in terms of the degrees of freedom for signal which is the trace of the averaging kernel. Mathematically this is the sum of the diagonal elements of the averaging kernel matrix (Rodgers, 2000).

Using the averaging kernel matrix leads to an alternative expression for the *optimal estimate* or *retrieval* $\hat{\mathbf{x}}$:

$$\hat{\mathbf{x}} = \mathbf{A}\mathbf{x} + (\mathbf{I}_n - \mathbf{A})\mathbf{x}_a + \mathbf{G}\epsilon \quad (16)$$

where \mathbf{I}_n is the identity matrix of dimension n . There are three terms on the right hand side of Equation 16. The first term, $\mathbf{A}\mathbf{x}$ represents the contribution of the true state \mathbf{x} to the solution. The second term $(\mathbf{I}_n - \mathbf{A})\mathbf{x}_a$ represents the contribution of the *a priori* assumptions. The third term $\mathbf{G}\epsilon$ is the contribution from random observational error. An ideal measurement would have an averaging kernel matrix that was an n dimensional identity matrix, $\mathbf{A} = \mathbf{I}_n$ in which case the 2nd term is zero (Jacob, 2007; Rodgers, 2000).

The second term in Equation 16, $[(In - A)_{x_a}]$ is called the *smoothing uncertainty* (since it results in a smoothing of the retrieval towards the *a priori* values). The third term, $G\epsilon$, is known as the *retrieval uncertainty* (or *signal-to-noise uncertainty*) but again it should be noted that this includes not only measurement noise but also errors in the forward model such as errors in the HITRAN database and that these factors often dominate the spectral noise. There may also be errors in the forward model that are correlated with one another and are therefore not random, potentially leading to uncharacterised biases in the retrievals. One other error that can be estimated is the *temperature uncertainty*, due to errors in the assumed temperature profile in the forward model. These lead to errors in the line strengths and resulting retrieved trace gas amounts that may be calculate using Equation 8.

5. A summary of past successes for ground-based solar Fourier transform infrared spectroscopy of atmospheric composition

In the late 1970's there were two groups of researchers actively engaged in making solar infrared measurements of atmospheric composition from the ground. The scientific focus at the time was on understanding the chemistry of the stratosphere and many measurements were made using balloon-borne grating spectrometers (Murcray *et al.*, 1975; Zander, 1976). Bradford *et al* (1976) outlined the feasibility of monitoring atmospheric trace gases using ground-based high resolution infrared spectroscopy. Within a couple of years the first scientific results from ground-based stations had been published, confirming the presence of hydrogen fluoride in the stratosphere from ground-based measurements from the Jungfraujoch in Switzerland, (47°N, 8.0°E) (Zander *et al.*, 1977) and identifying atmospheric absorption features of ammonia in spectra from Kitt peak in the USA, (32°N, 112°W) (Murcray *et al.*, 1978). In 1979 Goldman *et al*, published their "New Atlas of Infrared Solar Spectra" which included telluric absorption features of carbon dioxide, water, methane, carbon monoxide, nitrous oxide, ozone, carbonyl fluoride, chlorine nitrate, difluorochloromethane (CFC-22), dichlorodifluoromethane (CFC-12), sulphur hexafluoride and nitric acid as well as a number of absorption features from carbon monoxide and hydroxyl radicals in the solar atmosphere.

As the capabilities increased more trace gases were added to the list of measureable species including hydrogen cyanide (Rinsland *et al.*, 1982), nitric oxide (Rinsland *et al.*, 1984) and chlorine nitrate (Zander *et al.*, 1986). After the discovery of the Antarctic ozone hole (Farman *et al.*, 1985) and the establishment of the Network for Detection of Stratospheric Change (NDSC), the number of ground-based Fourier transform spectrometers making solar atmospheric absorption measurements increased dramatically. During the first half of the 1990's Fourier transform solar remote sensing spectrometers were installed at a number of new sites including Lauder, New Zealand (45°S, 170°E) in 1990 (Jones *et al.*, 1994); Mauna Loa, Hawaii (20°N, 156°W)(David *et al.*, 1993) & Arrival Heights, Antarctica (78°S, 167°E)(Kreher *et al.*, 1996; Wood *et al.*, 2004) in 1991, Ny Alesund, Spitzbergen (79°N, 12°E) in 1992 (Notholt and Schrems, 1994) and Harestua, Norway (60°N, 11°E) in 1994 (Mellqvist *et al.*, 2002). In 1994 the first measurements using the moon as a light source were reported from Spitzbergen, enabling measurements of the Arctic atmosphere during polar night (Notholt, 1994).

In 1995 three additional sites were added to the network at Zugspitze, Germany (47°N, 11°E) (Sussmann and Schafer, 1997), Rikubetsu, Japan (44°N, 144°E)(Zhao *et al.*, 2000) and Wollongong, Australia (34°S, 151°E) (Rinsland *et al.*, 2001). The following year saw a further

three sites established at Kiruna, Sweden, (68°N, 20°E) (*Blumenstock et al.*, 1997), Eureka, Nunavit (80°N, 86°W) (*Batchelor et al.*, 2009; *Donovan et al.*, 1997) and Moshiri, Japan (44°N, 142°E) (*Zhao et al.*, 2000). Measurements at Tsukuba, Japan (36°N, 140°E) started in 1998, followed by Thule, Greenland (77°N, 69°W), Poker Flat, Alaska (65°N, 147°W) and Izana, Tenerife Island (28°N, 16°W) all in 1999.

In the meanwhile there were a number of mobile instruments operating. The Jet Propulsion Laboratory's "Mark IV" instrument was making regular balloon flights from Alaska interspersed with ground-based measurements from Esrange (68°N, 21°E), Fairbanks (65°N, 148°W), Mount Barcroft (38°N, 118°W) or Table Mountain (34°N, 118°W) (*Toon et al.*, 1999b). The Alfred Wegner Institute had a ship-borne spectrometer onboard the Polarstern (*Notholt et al.*, 1995; *Notholt et al.*, 2000), and the National Physical Laboratory had a mobile instrument that made a series of side-by-side instrument intercomparisons with a number of other spectrometers in the network as well as a number of campaign measurements at Are, Sweden, Aberdeen, Scotland and Calar Alto, Spain (*Bell et al.*, 1994; *Bell et al.*, 1998; *Paton-Walsh et al.*, 1997). In addition to instrument intercomparisons, there were a number of algorithm intercomparison exercises and a standard procedure for characterising the instrument line-shape was developed (*Hase et al.*, 1999; *Hase et al.*, 2004). *A priori* profiles were most commonly based upon measurements from the balloon-based MarkIV instrument (*Toon et al.*, 1999a) or from the ATMOS instrument that was flown on the Space Shuttle (*Gunson et al.*, 1996).

Early in the new millennium the NDSC changed its name to the Network for Detection of Atmospheric Composition Change (NDACC) to highlight the change in scientific focus from stratospheric chemistry to changing tropospheric composition and greenhouse gases. The NDACC database (see <http://www.ndacc.org/>) contains standard gases for most stations equipped with a remote sensing FTIR spectrometer including ozone, nitric acid, hydrogen chloride, chlorine nitrate, hydrogen fluoride, nitrous oxide, carbon dioxide, carbon monoxide, methane, ethane and hydrogen cyanide. Many stations also provide other gases such as CFCs, nitrogen dioxide, nitrogen oxide and acetylene. Further stations were added including Toronto, Canada (44°N, 80°W) in 2002 and Bremen, Germany (53°N, 9°E) in 2004, whilst campaign measurements have been made at sites including Reunion Island, (22° S, 56°E) (*Senten et al.*, 2008), Paramaribo, Suriname (6°N, 55°W) (*Petersen et al.*, 2010) and Addis Ababa (9°N, 39°E). Further gases have also been identified in spectra from solar remote sensing Fourier transform spectrometers included chlorine monoxide (*Bell et al.*, 1996), formic acid, (*Rinsland et al.*, 2004), ethylene (*Rinsland et al.*, 2005) and methanol (*Paton-Walsh et al.*, 2008). In addition there have been a number of studies that examine different isotopes (*Frankenberg et al.*, 2009; *Goldman et al.*, 2000; *Goldman et al.*, 2002; *Haverd et al.*, 2005; *Irion et al.*, 1996; *Meier and Notholt*, 1996; *Notholt et al.*, 2010). Trends in both stratospheric gases eg (*Rinsland et al.*, 2003) and tropospheric gases eg (*Jones et al.*, 2009) have been established from NDACC remote sensing FTIR spectrometers. Recently there has been significant interest in the ability of this technique to characterise free tropospheric water vapour and its isotopes (*Palm et al.*, 2010; *Schneider et al.*, 2010). The NDACC continues to provide ground-validation for a number of retrieved products from several different satellite-based sensors (*Dils et al.*, 2006; *Dupuy et al.*, 2009; *Mahieu et al.*, 2008; *Payan et al.*, 2009; *Strong et al.*, 2008; *Vigouroux et al.*, 2007; *Wolff et al.*, 2008; *Yurganov et al.*, 2008).

In 2004 the Total Carbon Column Observing Network (TCCON) was established with the aim of making very accurate measurements of greenhouse gases in the near-infrared spectral region (see <https://tcon-wiki.caltech.edu/>). The primary function of TCCON was

to act as a network of ground-truthing stations for the Orbiting Carbon Observatory (Crisp *et al.*, 2004), however TCCON also had a remit to provide independent constraints to models of the carbon cycle and provide validation data to other satellite-based sensors. New sites were established at Park Falls, Wisconsin, USA (46°N, 90°W) (Washenfelder *et al.*, 2006) and Darwin, Australia (12°S, 131°E) (Deutscher *et al.*, 2009) whilst in a number of existing NDACC sites have been upgraded to allow for the extended spectral coverage and improved precision demanded for TCCON. The failure of the launch of the Orbiting Carbon Observatory has meant that TCCON has yet to fulfil its primary function however a re-launch is now planned and in the meanwhile TCCON has started to elucidate details of the carbon cycle itself (Yang *et al.*, 2007). More TCCON stations are being set-up and the data is available for the validation of other satellite instruments such as SCIAMACHY, AIRS, IASI and GOSAT (Bosch *et al.*, 2006).

6. Concluding remarks

Remote sensing of atmospheric trace gases by ground-based solar Fourier transform infrared spectroscopy has developed rapidly since its origins in the 1970s. It has had major successes in characterising the composition of the atmosphere and trends in both stratospheric and tropospheric gases. Whilst the technique has greater uncertainties than ground level *in situ* measurements of atmospheric composition, it characterises the total atmospheric column amount. Interpretation of ground level measurements is often complicated by the effects of vertical transport and changing boundary layer height, but total column measurements are less sensitive to this problem because the measurement is integrated over the whole atmosphere. A significant drawback to these remote sensing techniques is that they are numerically ill-posed and thus some *a priori* information is required to derive total column amounts from the spectra. In future atmospheric models are likely to be constrained by use of combined *in situ* and remotely sensed data such that the total uncertainties are minimised.

Remote sensing Fourier transform spectrometers play a vital role in our efforts to understand the changing composition of the atmosphere. The networks of ground-based instruments are continuing to expand, with improving precision & accuracy. These measurements will continue to improve our understanding of atmospheric composition and chemistry and provide ground validation for a new generation of satellite-based instruments.

7. References

- Barret, B., M. De Maziere, and E. Mahieu (2003), Ground-based FTIR measurements of CO from the Jungfraujoch: characterisation and comparison with *in situ* surface and MOPITT data, *Atmospheric Chemistry And Physics*, 3, 2217-2223.
- Batchelor, R. L., K. Strong, R. Lindenmaier, et al. (2009), A New Bruker IFS 125HR FTIR Spectrometer for the Polar Environment Atmospheric Research Laboratory at Eureka, Nunavut, Canada: Measurements and Comparison with the Existing Bomem DA8 Spectrometer, *Journal of Atmospheric and Oceanic Technology*, 26(7), 1328-1340.
- Bell, W., N. A. Martin, T. D. Gardiner, et al. (1994), Column Measurements of Stratospheric Trace Species over Are, Sweden in the Winter of 1991-1992, *Geophysical Research Letters*, 21(13), 1347-1350.

- Bell, W., C. Paton-Walsh, T. D. Gardiner, et al. (1996), Measurements of stratospheric chlorine monoxide (ClO) from groundbased FTIR observations, *Journal of Atmospheric Chemistry*, 24(3), 285-297.
- Bell, W., C. Paton-Walsh, T. D. Gardiner, et al. (1998), Ground-based FTIR measurements of stratospheric trace species from Aberdeen during winter and spring 1993/94 and 1994/95 and comparison with a 3D model, *Journal of Atmospheric Chemistry*, 30(1), 119-130.
- Blumenstock, T., H. Fischer, A. Friedle, et al. (1997), Column amounts of ClONO₂, HCl, HNO₃, and HF from ground-based FTIR measurements made near Kiruna, Sweden, in late winter 1994, *Journal of Atmospheric Chemistry*, 26(3), 311-321.
- Bosch, H., G. C. Toon, B. Sen, et al. (2006), Space-based near-infrared CO₂ measurements: Testing the Orbiting Carbon Observatory retrieval algorithm and validation concept using SCIAMACHY observations over Park Falls, Wisconsin, *Journal Of Geophysical Research-Atmospheres*, 111(D23).
- Bradford, C. M., F. H. Murcray, J. W. Vanallen, et al. (1976), GROUND LEVEL DETECTION AND FEASIBILITY FOR MONITORING OF SEVERAL TRACE ATMOSPHERIC CONSTITUENTS BY HIGH-RESOLUTION INFRARED SPECTROSCOPY, *Geophysical Research Letters*, 3(7), 387-390.
- Crisp, D., R. M. Atlas, F. M. Breon, et al. (2004), The orbiting carbon observatory (OCO) mission, in *Trace Constituents in the Troposphere and Lower Stratosphere*, edited by J. P. Burrows and A. M. Thompson, pp. 700-709, Pergamon-Elsevier Science Ltd, Kidlington.
- David, S. J., S. A. Beaton, M. H. Anderberg, et al. (1993), Determination of Total Ozone over Mauna-Loa Using Very High-Resolution Infrared Solar Spectra, *Geophysical Research Letters*, 20(19), 2055-2058.
- Deutscher, N. M., D. W. T. Griffith, G. W. Bryant, et al. (2009), Total column CO₂ measurements at Darwin, Australia - Site description and calibration against in situ aircraft profiles, *Journal of Geophysical Research*.
- Dils, B., M. De Maziere, J. F. Muller, et al. (2006), Comparisons between SCIAMACHY and ground-based FTIR data for total columns of CO, CH₄, CO₂ and N₂O, *Atmospheric Chemistry And Physics*, 6, 1953-1976.
- Donovan, D. P., H. Fast, Y. Makino, et al. (1997), Ozone, column ClO, and PSC measurements made at the NDSC Eureka observatory (80 degrees N, 86 degrees W) during the spring of 1997, *Geophysical Research Letters*, 24(22), 2709-2712.
- Dupuy, E., K. A. Walker, J. Kar, et al. (2009), Validation of ozone measurements from the Atmospheric Chemistry Experiment (ACE), *Atmospheric Chemistry And Physics*, 9(2), 287-343.
- Farman, J. C., B. G. Gardiner, and J. D. Shanklin (1985), Large Losses of Total Ozone in Antarctica Reveal Seasonal ClOx/Nox Interaction, *Nature*, 315(6016), 207-210.
- Frankenberg, C., K. Yoshimura, T. Warneke, et al. (2009), Dynamic Processes Governing Lower-Tropospheric HDO/H₂O Ratios as Observed from Space and Ground, *Science*, 325(5946), 1374-1377.
- Goldman, A., R. D. Blatherwick, F. H. Murcray, et al. (1979), NEW ATLAS OF IR SOLAR SPECTRA, *Applied Optics*, 18(5), 604-605.

- Goldman, A., M. T. Coffey, T. M. Stephen, et al. (2000), Isotopic OCS from high-resolution balloon-borne and ground-based infrared solar absorption spectra, *Journal of Quantitative Spectroscopy & Radiative Transfer*, 67(6), 447-455.
- Goldman, A., C. P. Rinsland, A. Perrin, et al. (2002), Weak ozone isotopic absorption in the 5 μ m region from high resolution FTIR solar spectra, *Journal of Quantitative Spectroscopy & Radiative Transfer*, 74(1), 133-138.
- Griffith, D. W. T. (1996), Synthetic calibration and quantitative analysis of gas phase infrared spectra, *Applied Spectroscopy*, 50(1), 59-70.
- Gunson, M. R., M. M. Abbas, M. C. Abrams, et al. (1996), The Atmospheric Trace Molecule Spectroscopy (ATMOS) experiment: Deployment on the ATLAS Space Shuttle missions, *Geophysical Research Letters*, 23(17), 2333-2336.
- Hase, F., T. Blumenstock, and C. Paton-Walsh (1999), Analysis of the instrumental line shape of high-resolution Fourier transform IR spectrometers with gas cell measurements and new retrieval software, *Applied Optics*, 38(15), 3417-3422.
- Hase, F., J. W. Hannigan, M. T. Coffey, et al. (2004), Intercomparison of retrieval codes used for the analysis of high-resolution, ground-based FTIR measurements, *Journal of Quantitative Spectroscopy & Radiative Transfer*, 87(1), 25-52.
- Haverd, V., G. C. Toon, and D. W. T. Griffith (2005), Evidence for altitude-dependent photolysis-induced O-18 isotopic fractionation in stratospheric ozone, *Geophysical Research Letters*, 32(22), 4.
- Irion, F. W., M. R. Gunson, C. P. Rinsland, et al. (1996), Heavy ozone enrichments from ATMOS infrared solar spectra, *Geophysical Research Letters*, 23(17), 2377-2380.
- Jacob, D. J. (2007), Lectures on Inverse Modeling, edited.
- Jones, N. B., M. Koike, W. A. Matthews, et al. (1994), Southern Hemisphere Seasonal Cycle in total column Nitric Acid, *Geophys. Res. Lett.*, 21(7), 593-596.
- Jones, N. B., K. Riedel, W. Allan, et al. (2009), Long-term tropospheric formaldehyde concentrations deduced from ground-based fourier transform solar infrared measurements, *Atmospheric Chemistry And Physics*, 9(18), 7131-7142.
- Kreher, K., J. G. Keys, P. V. Johnston, et al. (1996), Ground-based measurements of OClO and HCl in austral spring 1993 at Arrival Heights, Antarctica, *Geophysical Research Letters*, 23(12), 1545-1548.
- Mahieu, E., C. P. Rinsland, R. Zander, et al. (1995), Vertical Column Abundances of HCN Deduced from Ground-Based Infrared Solar Spectra - Long-Term Trend and Variability, *Journal of Atmospheric Chemistry*, 20(3), 299-310.
- Mahieu, E., P. Duchatelet, P. Demoulin, et al. (2008), Validation of ACE-FTS v2.2 measurements of HCl, HF, CCl₃F and CCl₂F₂ using space-, balloon- and ground-based instrument observations, *Atmospheric Chemistry And Physics*, 8(20), 6199-6221.
- Meier, A., and J. Notholt (1996), Determination of the isotopic abundances of heavy O-3 as observed in arctic ground-based FTIR-spectra, *Geophysical Research Letters*, 23(5), 551-554.
- Meier, A., A. Goldman, P. Manning, et al. (2003), Improvements to Air Mass Calculations for Ground-Based Infrared Measurements, *J. Quant. Spectrosc. Radiat. Transfer*, doi:10.1016/S0022-4073(02)00018-3.
- Meier, A., G. Toon, C. Rinsland, et al. (2004), Spectroscopic Atlas of Atmospheric Microwindows in the Middle Infra-red, Institutet for Rymdfysik, Kiruna, Sweden.

- Mellqvist, J., B. Galle, T. Blumenstock, et al. (2002), Ground-based FTIR observations of chlorine activation and ozone depletion inside the Arctic vortex during the winter of 1999/2000, *Journal Of Geophysical Research-Atmospheres*, 107(D20).
- Migeotte, M. V. (1948), Spectroscopic evidence of methane in the earth's atmosphere, *Phys Rev*, 73, 519-520.
- Migeotte, M. V. (1949), The fundamental band of carbon monoxide at 4.7 microns in the solar spectrum, *Phys Rev*, 75, 1108-1109.
- Murcray, D. G., F. S. Bonomo, J. N. Brooks, et al. (1975), DETECTION OF FLUOROCARBONS IN STRATOSPHERE, *Geophysical Research Letters*, 2(3), 109-112.
- Murcray, D. G., A. Goldman, C. M. Bradford, et al. (1978), IDENTIFICATION OF NU-2 VIBRATION-ROTATION BAND OF AMMONIA IN GROUND LEVEL SOLAR SPECTRA, *Geophysical Research Letters*, 5(6), 527-530.
- Nagahama, Y., and K. Suzuki (2007), The influence of forest fires on CO, HCN, C₂H₆, and C₂H₂ over northern Japan measured by infrared solar spectroscopy, *Atmospheric Environment*, 41(40), 9570-9579.
- Notholt, J. (1994), The Moon as a Light-Source for Ftir Measurements of Stratospheric Trace Gases During the Polar Night - Application for Hno₃ in the Arctic, *Journal Of Geophysical Research-Atmospheres*, 99(D2), 3607-3614.
- Notholt, J., and O. Schrems (1994), GROUND-BASED FTIR MEASUREMENTS OF VERTICAL COLUMN DENSITIES OF SEVERAL TRACE GASES ABOVE SPITSBERGEN, *Geophysical Research Letters*, 21(13), 1355-1358.
- Notholt, J., I. Beninga, and O. Schrems (1995), SHIP-BORNE FT-IR MEASUREMENTS OF ATMOSPHERIC TRACE GASES ON A SOUTH (33-DEGREES-S) TO NORTH (53-DEGREES-N) ATLANTIC TRAVERSE, *Applied Spectroscopy*, 49(10), 1525-1527.
- Notholt, J., G. C. Toon, C. P. Rinsland, et al. (2000), Latitudinal variations of trace gas concentrations in the free troposphere measured by solar absorption spectroscopy during a ship cruise, *Journal Of Geophysical Research-Atmospheres*, 105(D1), 1337-1349.
- Notholt, J., G. C. Toon, S. Fueglistaler, et al. (2010), Trend in ice moistening the stratosphere - constraints from isotope data of water and methane, *Atmospheric Chemistry And Physics*, 10(1), 201-207.
- Palm, M., C. Melsheimer, S. Noel, et al. (2010), Integrated water vapor above Ny Alesund, Spitsbergen: a multi-sensor intercomparison, *Atmospheric Chemistry And Physics*, 10(3), 1215-1226.
- Paton-Walsh, C., W. Bell, T. Gardiner, et al. (1997), An uncertainty budget for ground-based Fourier transform infrared column measurements of HCl, HF, N₂O, and HNO₃, deduced from results of side-by-side instrument intercomparisons, *Journal Of Geophysical Research-Atmospheres*, 102(D7), 8867-8873.
- Paton-Walsh, C., S. R. Wilson, N. B. Jones, et al. (2008), Measurement of methanol emissions from Australian wildfires by ground-based solar Fourier transform spectroscopy, *Geophysical Research Letters*, 35(8).
- Payan, S., C. Camy-Peyret, H. Oelhaf, et al. (2009), Validation of version-4.61 methane and nitrous oxide observed by MIPAS, *Atmospheric Chemistry And Physics*, 9(2), 413-442.

- Petersen, A. K., T. Warneke, C. Frankenberg, et al. (2010), First ground-based FTIR observations of methane in the inner tropics over several years, *Atmospheric Chemistry And Physics*, 10(15), 7231-7239.
- Pougatchev, N. S., B. J. Connor, and C. P. Rinsland (1995), Infrared measurements of the ozone vertical-distribution above Kitt Peak, *Journal Of Geophysical Research-Atmospheres*, 100(D8), 16689-16697.
- Rinsland, C. P., M. A. H. Smith, P. L. Rinsland, et al. (1982), Ground-based infrared spectroscopic measurements of atmospheric hydrogen-cyanide, *Journal Of Geophysical Research-Oceans and Atmospheres*, 87(NC13), 1119-1125.
- Rinsland, C. P., R. E. Boughner, J. C. Larsen, et al. (1984), Diurnal-variations of atmospheric nitric-oxide - ground-based infrared spectroscopic measurements and their interpretation with time-dependent photochemical model-calculations, *Journal Of Geophysical Research-Atmospheres*, 89(ND6), 9613-9622.
- Rinsland, C. P., R. Zander, L. R. Brown, et al. (1986), Detection of Carbonyl Fluoride in the Stratosphere, *Geophysical Research Letters*, 13(8), 769-772.
- Rinsland, C. P., N. B. Jones, B. J. Connor, et al. (1998), Northern and Southern Hemisphere Ground-Based Infrared Spectroscopic Measurements of Tropospheric Carbon Monoxide and Ethane, *Journal of Geophysical Research*, 103, 28,197-128,218.
- Rinsland, C. P., E. Mahieu, R. Zander, et al. (2000), Free tropospheric CO, C₂H₆, and HCN above central Europe: Recent measurements from the Jungfraujoch station including the detection of elevated columns during 1998, *Journal Of Geophysical Research-Atmospheres*, 105(D19), 24235-24249.
- Rinsland, C. P., A. Meier, D. W. T. Griffith, et al. (2001), Ground-based measurements of tropospheric CO, C₂H₆, and HCN from Australia at 34 degrees S latitude during 1997-1998, *Journal Of Geophysical Research-Atmospheres*, 106(D18), 20913-20924.
- Rinsland, C. P., A. Goldman, E. Mahieu, et al. (2002), Ground-based infrared spectroscopic measurements of carbonyl sulfide: Free tropospheric trends from a 24-year time series of solar absorption measurements, *Journal Of Geophysical Research-Atmospheres*, 107(D22), -.
- Rinsland, C. P., E. Mathieu, R. Zander, et al. (2003), Long-term trends of inorganic chlorine from ground-based infrared solar spectra: Past increases and evidence for stabilization, *Journal Of Geophysical Research-Atmospheres*, 108(D8), 21.
- Rinsland, C. P., E. Mahieu, R. Zander, et al. (2004), Free tropospheric measurements of formic acid (HCOOH) from infrared ground-based solar absorption spectra: Retrieval approach, evidence for a seasonal cycle, and comparison with model calculations, *Journal Of Geophysical Research-Atmospheres*, 109(D18).
- Rinsland, C. P., C. Paton-Walsh, N. B. Jones, et al. (2005), High spectral resolution solar absorption measurements of ethylene (C₂H₄) in a forest fire smoke plume using HITRAN parameters: Tropospheric vertical profile retrieval, *Journal Of Quantitative Spectroscopy and Radiative Transfer*, 96(2), 301.
- Rinsland, C. P., L. Chiou, E. Mahieu, et al. (2008), Measurements of long-term changes in atmospheric OCS (carbonyl sulfide) from infrared solar observations, *Journal of Quantitative Spectroscopy & Radiative Transfer*, 109(16), 2679-2686.
- Rodgers, C. D. (1990), Characterization and error analysis of profiles retrieved from remote sounding measurements, *Journal of Geophysical Research*, 95, 5587-5595.

- Rodgers, C. D. (2000), *Inverse Methods for Atmospheric Sounding: Theory and Practice*, World Scientific Publishing Co. Pte. Ltd, New Jersey.
- Rothman, L. S., C. P. Rinsland, A. Goldman, et al. (1998), The HITRAN molecular spectroscopic database and HAWKS (HITRAN Atmospheric Workstation): 1996 edition, *Journal of Quantitative Spectroscopy & Radiative Transfer*, 60(5), 665-710.
- Rothman, L. S., A. Barbe, D. C. Benner, et al. (2003), The HITRAN molecular spectroscopic database: edition of 2000 including updates through 2001, *Journal of Quantitative Spectroscopy & Radiative Transfer*, 82(1-4), 5-44.
- Rothman, L. S., D. Jacquemart, A. Barbe, et al. (2005), The HITRAN 2004 molecular spectroscopic database, *Journal of Quantitative Spectroscopy & Radiative Transfer*, 96(2), 139-204.
- Schneider, M., K. Yoshimura, F. Hase, et al. (2010), The ground-based FTIR network's potential for investigating the atmospheric water cycle, *Atmospheric Chemistry And Physics*, 10(7), 3427-3442.
- Senten, C., M. De Maziere, B. Dils, et al. (2008), Technical note: New ground-based FTIR measurements at Ile de La Reunion: observations, error analysis, and comparisons with independent data, *Atmospheric Chemistry And Physics*, 8(13), 3483-3508.
- Strong, K., M. A. Wolff, T. E. Kerzenmacher, et al. (2008), Validation of ACE-FTS N₂O measurements, *Atmospheric Chemistry And Physics*, 8(16), 4759-4786.
- Sussmann, R., and K. Schafer (1997), Infrared spectroscopy of tropospheric trace gases: Combined analysis of horizontal and vertical column abundances, *Applied Optics*, 36(3), 735-741.
- Toon, G. C., J. F. Blavier, B. Sen, et al. (1999a), Comparison of MkIV balloon and ER-2 aircraft measurements of atmospheric trace gases, *Journal Of Geophysical Research-Atmospheres*, 104(D21), 26779-26790.
- Toon, G. C., J. F. Blavier, B. Sen, et al. (1999b), Ground-based observations of Arctic O₃ loss during spring and summer 1997, *Journal Of Geophysical Research-Atmospheres*, 104(D21), 26497-26510.
- Vigouroux, C., M. De Maziere, Q. Errera, et al. (2007), Comparisons between ground-based FTIR and MIPAS N₂O and HNO₃ profiles before and after assimilation in BASCOE, *Atmospheric Chemistry And Physics*, 7, 377-396.
- Warneke, T., J. F. Meirink, P. Bergamaschi, et al. (2006), Seasonal and latitudinal variation of atmospheric methane: A ground-based and ship-borne solar IR spectroscopic study, *Geophysical Research Letters*, 33(14).
- Washenfelder, R. A., G. C. Toon, J. F. Blavier, et al. (2006), Carbon dioxide column abundances at the Wisconsin Tall Tower site, *Journal Of Geophysical Research-Atmospheres*, 111(D22).
- Wolff, M. A., T. Kerzenmacher, K. Strong, et al. (2008), Validation of HNO₃, ClONO₂, and N₂O₅ from the Atmospheric Chemistry Experiment Fourier Transform Spectrometer (ACE-FTS), *Atmospheric Chemistry And Physics*, 8(13), 3529-3562.
- Wood, S. W., R. L. Batchelor, A. Goldman, et al. (2004), Ground-based nitric acid measurements at Arrival Heights, Antarctica, using solar and lunar Fourier transform infrared observations, *Journal Of Geophysical Research-Atmospheres*, 109(D18).
- Yang, Z., R. A. Washenfelder, G. Keppel-Aleks, et al. (2007), New constraints on Northern Hemisphere growing season net flux, *Geophysical Research Letters*, 34(12), 6.

- Yurganov, L. N., W. W. McMillan, A. V. Dzhola, et al. (2008), Global AIRS and MOPITT CO measurements: Validation, comparison, and links to biomass burning variations and carbon cycle, *Journal Of Geophysical Research-Atmospheres*, 113(D9).
- Zander, R. (1976), HIGH-RESOLUTION INFRARED SOLAR OBSERVATIONS BY BALLOON, *Infrared Physics*, 16(1-2), 125-127.
- Zander, R., G. Roland, and L. Delbouille (1977), CONFIRMING PRESENCE OF HYDROFLUORIC-ACID IN UPPER STRATOSPHERE, *Geophysical Research Letters*, 4(3), 117-120.
- Zander, R., C. P. Rinsland, C. B. Farmer, et al. (1986), Observation of Several Chlorine Nitrate (ClONO₂) Bands in Stratospheric Infrared-Spectra, *Geophysical Research Letters*, 13(8), 757-760.
- Zhao, Y., Y. Kondo, F. J. Murcray, et al. (2000), Seasonal variations of HCN over northern Japan measured by ground-based infrared solar spectroscopy, *Geophysical Research Letters*, 27(14), 2085-2088.
- Zhao, Y., K. Strong, Y. Kondo, et al. (2002), Spectroscopic measurements of tropospheric CO, C₂H₆, C₂H₂, and HCN in northern Japan, *Journal Of Geophysical Research-Atmospheres*, 107(D18), -.

IntechOpen



Fourier Transforms - New Analytical Approaches and FTIR Strategies

Edited by Prof. Goran Nikolic

ISBN 978-953-307-232-6

Hard cover, 520 pages

Publisher InTech

Published online 01, April, 2011

Published in print edition April, 2011

New analytical strategies and techniques are necessary to meet requirements of modern technologies and new materials. In this sense, this book provides a thorough review of current analytical approaches, industrial practices, and strategies in Fourier transform application.

How to reference

In order to correctly reference this scholarly work, feel free to copy and paste the following:

Clare Paton-Walsh (2011). Remote Sensing of Atmospheric Trace Gases by Ground-Based Solar Fourier Transform Infrared Spectroscopy, *Fourier Transforms - New Analytical Approaches and FTIR Strategies*, Prof. Goran Nikolic (Ed.), ISBN: 978-953-307-232-6, InTech, Available from:

<http://www.intechopen.com/books/fourier-transforms-new-analytical-approaches-and-ftir-strategies/remote-sensing-of-atmospheric-trace-gases-by-ground-based-solar-fourier-transform-infrared-spectrosc>

INTECH
open science | open minds

InTech Europe

University Campus STeP Ri
Slavka Krautzeka 83/A
51000 Rijeka, Croatia
Phone: +385 (51) 770 447
Fax: +385 (51) 686 166
www.intechopen.com

InTech China

Unit 405, Office Block, Hotel Equatorial Shanghai
No.65, Yan An Road (West), Shanghai, 200040, China
中国上海市延安西路65号上海国际贵都大饭店办公楼405单元
Phone: +86-21-62489820
Fax: +86-21-62489821

© 2011 The Author(s). Licensee IntechOpen. This chapter is distributed under the terms of the [Creative Commons Attribution-NonCommercial-ShareAlike-3.0 License](#), which permits use, distribution and reproduction for non-commercial purposes, provided the original is properly cited and derivative works building on this content are distributed under the same license.

IntechOpen

IntechOpen